doi:10.1093/brain/aws028 Brain 2012: 135; 1055–1069 | 1055

BRAIN
A JOURNAL OF NEUROLOGY

# Interferon regulatory factor 7 regulates glioma stem cells via interleukin-6 and Notch signalling

Xun Jin,[1,*] Sung-Hak Kim,[1,*] Hye-Min Jeon,[1,*] Samuel Beck,[2] Young-Woo Sohn,[1] Jinlong Yin,[2] Jun-Kyum Kim,[1] Young Chang Lim,[3] Jun-Han Lee,[4] Se-Hyuk Kim,[5] Shin-Hyuk Kang,[6] Xumin Pian,[1] Min-Suk Song,[4] Jong Bae Park,[7] Yang-Seok Chae,[8] Yong-Gu Chung,[6] Seung-Hoon Lee,[7] Yun-Jaie Choi,[2] Do-Hyun Nam,[9] Young Ki Choi[4] and Hyunggee Kim[1]

1 School of Life Sciences and Biotechnology, Korea University, Seoul 136–713, Republic of Korea
2 School of Agricultural Biotechnology, Seoul National University, Seoul 151–921, Republic of Korea
3 Department of Otorhinolaryngology-Head and Neck Surgery, Research Institute of Medical Science, Konkuk University School of Medicine, Seoul 143–729, Republic of Korea
4 College of Medicine and Medical Research Institute, Chungbuk National University, Chongju 361–763, Republic of Korea
5 Department of Neurosurgery, School of Medicine, Ajou University, Suwon 443–721, Republic of Korea
6 Department of Neurosurgery, College of Medicine, Korea University, Seoul 136–705, Republic of Korea
7 Specific Organs Cancer Division, Research Institute and Hospital, National Cancer Centre, Goyang 410–769, Republic of Korea
8 Department of Pathology, College of Medicine, Korea University, Seoul 136–705, Republic of Korea
9 Department of Neurosurgery, Samsung Medical Centre and Samsung Biomedical Research Institute, Sungkyunkwan University School of Medicine, Seoul 135–710, Republic of Korea

*These authors contributed equally to this work.

Correspondence to: Hyunggee Kim, PhD,
School of Life Sciences and Biotechnology,
Korea University,
5-ga, Anam-dong, Seongbuk-gu,
Seoul 136-713, Republic of Korea
E-mail: hg-kim@korea.ac.kr

**Inflammatory microenvironment signalling plays a crucial role in tumour progression (i.e. cancer cell proliferation, survival, angiogenesis and metastasis) in many types of human malignancies. However, the role of inflammation in brain tumour pathology remains poorly understood. Here, we report that interferon regulatory factor 7 is a crucial regulator of brain tumour progression and heterogeneity. Ectopic expression of interferon regulatory factor 7 in glioma cells promotes tumorigenicity, angiogenesis, microglia recruitment and cancer stemness *in vivo* and *in vitro* through induction of interleukin 6, C-X-C motif chemokine 1 and C–C motif chemokine 2. In particular, interferon regulatory factor 7-driven interleukin 6 plays a pivotal role in maintaining glioma stem cell properties via Janus kinase/signal transducer and activator of transcription-mediated activation of Jagged-Notch signalling in glioma cells and glioma stem cells derived from glioma patients. Accordingly, the short hairpin RNA-mediated depletion of interferon regulatory factor 7 in glioma stem cells markedly suppressed interleukin 6-Janus kinase/signal transducer and activator of transcription-mediated Jagged-Notch-signalling pathway, leading to decreases in glioma stem cell marker expression, tumoursphere-forming ability, and tumorigenicity. Furthermore, in a mouse model of**

Received May 31, 2011. Revised November 23, 2011. Accepted December 19, 2011. Advance Access publication March 20, 2012

**wound healing, depletion of interferon regulatory factor 7 suppressed tumour progression and decreased cellular heterogeneity. Finally, interferon regulatory factor 7 was overexpressed in patients with high-grade gliomas, suggesting its potential as an independent prognostic marker for glioma progression. Taken together, our findings indicate that interferon regulatory factor 7-mediated inflammatory signalling acts as a major driver of brain tumour progression and cellular heterogeneity via induction of glioma stem cell genesis and angiogenesis.**

**Keywords:** glioma stem cells; angiogenesis; interferon regulatory factor 7; interleukin 6; tumour microenvironment

**Abbreviations:** CCL2 = C–C motif chemokine 2; CXCL1 = C-X-C motif chemokine 1; GSC = glioma stem cell; IL6 = interleukin 6; IRF7 = interferon regulatory factor 7; JAK = Janus kinase; shRNA = short hairpin RNA; STAT = signal transducer and activator of transcription; TNF$\alpha$ = tumour necrosis factor $\alpha$

# Introduction

Accumulating evidence from studies of many types of malignancies indicates that inflammatory signals regulated by cytokines and chemokines play critical roles in tumour progression (i.e. cancer cell proliferation, survival, angiogenesis and metastasis) (Coffelt *et al*., 2009). Therefore, inflammation in the microenvironment may be considered the seventh hallmark of cancer in addition to the six classical hallmarks (Mantovani *et al*., 2008, 2009). Although inflammation has long been suspected to be involved in brain tumour progression, direct evidence demonstrating its role in brain tumour pathology has been lacking.

The nine members of the interferon regulatory factor (IRF) family are transcription factors that play diverse roles in inflammatory responses including antiviral defence, cell proliferation and immune cell maturation (Honda *et al*., 2006). In particular, IRF7, which is a master regulator of type I interferon-dependent immune responses (Honda *et al*., 2005), was found to be over-expressed in paediatric lymphoma specimens (Park *et al*., 2007). In addition, ectopic expression of IRF7 in immortal NIH 3T3 mouse embryonic fibroblasts leads to *in vitro* transformation and *in vivo* tumour formation (Zhang *et al*., 2004).

Recently, several lines of evidence have suggested that the growth of glioblastoma multiforme is driven by glioma stem cells (GSCs) that display the molecular and cellular characteristics of normal neural stem cells. These shared properties include extensive self-renewal (i.e. continuous proliferation while maintaining an undifferentiated state) and a multi-differentiation potential (i.e. ability to produce a heterogeneous population of differentiated cells) (Stiles and Rowitch, 2008). However, the signalling pathways governing GSC genesis and glioma progression are not well understood and are under intensive investigation.

The pleiotropic nature of inflammation regulated by cytokines and IRFs led us to hypothesize that certain IRFs over-expressed in brain tumours may function as modulators of glioma progression. Here we reveal that a novel inflammatory response mediated by the IRF7–interleukin 6 (IL6) signalling axis plays a crucial role in brain tumour progression by generating an inflammatory microenvironment that enables glioma cells to acquire GSC properties.

# Materials and methods

## Cell culture and reagents

Human BJ fibroblast cells, human glioma cell lines (A172, A1207, LN18, LN229, T98G, U87MG and U138MG), and primary human brain vascular endothelial cells were purchased from the American Type Culture Collection. Normal human astrocytes and neural stem cells were purchased from Cambrex Bio Science. Human BJ fibroblast cells, human glioma cell lines, normal human astrocytes and murine microglial cells were maintained in high-glucose Dulbecco's modified Eagle's medium supplemented with 10% foetal bovine serum (HyClone), 1% penicillin and streptomycin (Life Technologies) and 2 mM L-glutamine (Life Technologies). Human brain vascular endothelial cells were grown in endothelial cell medium (Clonetics). All GSCs tested here were cultured using Neurobasal® medium (Invitrogen) supplemented with modified N2, B27, epidermal growth factor (20 ng/ml; R&D Systems) and basic fibroblast growth factor (20 ng/ml; R&D Systems) in suspension or in an adherent culture with laminin-coated flasks as described previously (Pollard *et al*., 2009). Cells were treated with pyridone 6 (0.5 μM; Calbiochem; Pedranzini *et al*., 2006), STAT3 inhibitor peptide (265 μM; Calbiochem; Turkson *et al*., 2001) and DAPT (100 nM; Sigma; Zheng *et al*., 2008) as indicated for 2 weeks to monitor tumoursphere-forming activity.

## Proliferation assay

For cell proliferation, $2.5 \times 10^4$ cells were plated in six-well dishes. The cells were harvested by trypsin digestion and counted using a haemocytometer on Days 1, 3 and 5.

## Plasmids, short hairpin RNA construction and transduction

To generate IRF7- and IL6-overexpressing cell lines, glioma cells were transduced with pcDNA3.1-IRF7.1-puro, pcDNA3.1-IL6 and pcDNA3.1-puro (control) using Lipofectamine™ 2000 (Invitrogen). To generate gene knockdown cell lines, glioma cells were transfected with retroviral vectors that express short hairpin RNA (shRNA) against the target genes [pSUPER.retro-shScramble (control), pSUPER.retro-shIRF7, pSUPER.retro-shIL6, pSUPER.retro-shCXCL1 and pSUPER.retro-shCCL2; OligoEngine]. GSCs were transduced with pSUPER.retro-shScramble and pSUPER.retro-shIRF7 using a microporation kit (Invitrogen). The target sequences were human IRF7-shRNA1 (5′-acccagtctaatgagaactc-3′), human IRF7-shRNA2 (5′-aacagcctcta

tgacgacatc-3′), human IL6-shRNA (5′-agatggatgcttccaatctgg-3′), human CXCL1-shRNA (5′-gctcactggtggctgttcct-3′), human CCL2-shRNA (5′-aaccacagttctacccct-3′) and scramble shRNA (5′-agacgga ggcttacagtctgg-3′).

## RNA and protein analyses

Reverse transcriptase–polymerase chain reaction analyses were performed to determine messenger RNA levels. Total RNA was isolated from cells using TRIzol® reagent (Invitrogen) and transcribed using a complementary DNA synthesis kit (Fermentas) according to the manufacturers' instructions. For semi-quantitative reverse transcriptase–polymerase chain reaction, 1 μl complementary DNA was used to amplify IRF7, IL6, C–C motif chemokine 2 (CCL2), C-X-C motif chemokine 1 (CXCL1), 18S ribosomal RNA, and glyceraldehyde 3-phosphate dehydrogenase (GAPDH) using gene-specific primer sets. Quantitative real-time polymerase chain reaction was performed on an iCycler IQ™ real-time detection system (Bio-Rad) using IQ™ Supermix with SYBR® Green (Bio-Rad), and data were analysed on the basis of threshold cycle values of each sample and normalized with 18S ribosomal RNA. Polymerase chain reaction primer information is shown in Supplementary Table 1. For western blot analysis, cells were collected with RIPA lysis buffer [150 mM NaCl, 1% NP-40, 0.1% sodium dodecyl sulphate and 50 mM Tris (pH 7.4)] containing 1 mM β-glycerophosphate, 2.5 mM sodium pyrophosphate, 1 mM NaF, 1 mM $Na_3VO_4$ and protease inhibitor (Roche). Samples were incubated on ice for 20 min, and supernatants were recovered by centrifugation at 14 000 rpm at 4°C. Protein concentrations were determined by the Bradford method (Bio-Rad). Proteins were separated by sodium dodecyl sulphate–polyacrylamide gel electrophoresis and transferred to polyvinylidene fluoride membranes (Upstate). The membranes were incubated with primary antibodies against IRF7, Jagged-1, cleaved Notch1, phosphorylated STAT3, STAT3, Hes1, Hey1, β-actin and α-tubulin (Supplementary Table 2). After removing the primary antibody, the membranes were incubated with horseradish peroxidase-conjugated secondary antibodies for 1 h. The signals were visualized by incubating the blots with enhanced chemiluminescence substrate (Pierce) and exposing to X-ray film (Agfa). Cytokines secreted into the cell culture media were quantified with an angiogenesis antibody array kit (RayBiotech), according to the manufacturer's instructions. The complete array maps (Array1) can be found at http://www.raybiotech.com/map_all_m.asp#8. Secreted IL6 was quantified using a human IL6 enzyme-linked immunosorbent assay kit (R&D Systems). The array was scanned and the signal intensity was analysed using ImageJ software (http://rsb.info.nih.gov/ij/).

## Immunofluorescence and immunohistochemistry assays

Human glioma specimens were collected from patients who had provided informed consent. The tissue collection protocol was approved by the institutional review board for human research at the Ajou University School of Medicine, Samsung Seoul Hospital and Sungkyunkwan University, Republic of Korea. Tumour tissue sections obtained from mouse xenografts and patients with glioma were incubated with IRF7, IL6, CD31, CD133, Nestin, S100β, Tuj1 and F4/80 antibodies. The stained sections were then examined using optical and confocal microscopy (Zeiss). Quantification of immunofluorescence staining was determined using MetaMorph® software (Molecular Devices). To quantify vessel areas in xenograft tumours driven by U87MG-puro, U87MG-IRF7, LN229-shScramble and LN229-shIRF7 cells, we determined the CD31-positive areas in three random fields. Cell populations positive for CD133, Nestin, S100β, Tuj1 or F4/80 revealed by immunohistochemistry or immunofluorescence were quantified by counting the number of positively stained cells of 100 nuclei in five randomly chosen high-power fields. The tumour volume was recorded (largest width$^2$ × largest length × 0.5). Antibody information is shown in Supplementary Table 2.

## Chromatin immunoprecipitation and luciferase reporter gene assays

The nuclear factor kappa B (NFκB), IRF7 and IRF3 response elements on the CXCL1, IL6 and CCL2 promoters were selected according to the web-based information and results of a previous study (http://www.sabiosciences.com/chipqpcrsearch.php; Panne *et al*., 2007). The chromatin immunoprecipitation assay (Upstate) was performed according to the manufacturer's protocol as described previously (Kim *et al*., 2007). Cells were fixed with 1% formaldehyde, suspended in sodium dodecyl sulphate lysis buffer and then sonicated. Immunoprecipitation was performed using antibodies against IRF7, IRF3, NFκB and mouse IgG (Pierce). The eluted DNA was purified using the Qiagen polymerase chain reaction purification kit and analysed by semi-quantitative reverse transcriptase–polymerase chain reaction and quantitative real-time polymerase chain reaction. The primers used for chromatin immunoprecipitation, which amplify specific upstream regions of each promoter, are shown in Supplementary Table 3. Promoter activity was determined in 293T cells after transfection of pGL3-IL6, pGL3-Jagged1 and pGL3-CSL promoter reporter plasmids using the Dual-Glo Luciferase Assay System (Promega). Transfection efficiency was determined by normalizing the reporter activity with *Renilla* luciferase activity according to the manufacturer's instructions (Promega).

## *In vitro* tube formation assay

*In vitro* tube formation of human brain vascular endothelial cells was evaluated using an *in vitro* angiogenesis assay kit (Chemicon). The U87MG-puro-shScramble, U87MG-CXCL1-shScramble, U87MG-IL6-shScramble, U87MG-CCL2-shScramble, U87MG-IRF7-shScramble, U87MG-IRF7-shCXCL1, U87MG-IRF7-shIL6 and U87MG-IRF7-shCCL2 cells were seeded at $5 \times 10^5$ cells per 10-cm plate. After 24-h incubation, the conditioned medium was harvested and filtered through a 0.2-μm filter (Sartorius Stedim Biotech). Endothelial cells were seeded in each well ($1 \times 10^4$ cells/well) and cultured in each type of conditioned medium at 37°C for 12 h. The cultures were then photographed (×40 magnification). Three random view fields per well were examined, and the tubes were counted.

## *In vitro* migration assay

Human brain vascular endothelial cells or microglial cells ($3 \times 10^4$) suspended in endothelial cell medium or starvation medium were added to the upper chamber (insert) of a migration chamber (3-μm pore size; Corning). The insert was then placed in a 24-well dish containing conditioned medium obtained from the indicated cell lines. The migrated cells were counted after 48 h.

## Tumoursphere-forming assay

Cells were seeded in 12-well plates (200 cells/well) in Neurobasal® medium supplemented with N2, B27, epidermal growth factor and basic fibroblast growth factor. The epidermal growth factor and

basic fibroblast growth factor were replaced every 3 days, and the number of tumourspheres was determined after 14 days. For the culture of three consecutive passages, tumourspheres were attached onto laminin-coated flasks and enzymatically dissociated between passages using Accutase® (Sigma).

## Fluorescence-activated cell sorting analysis

To determine proportions of cells positive for CD133, Nestin, Sox2, GFAP, S100β, Tuj1 and NG2, the dissociated cells were fixed with 4% paraformaldehyde and then permeabilized with 0.1% saponin. The cells were incubated with anti-CD133, anti-Nestin, anti-Sox2, anti-GFAP, anti-S100β, anti-Tuj1 and anti-NG2 antibodies, followed by incubation with biotin-conjugated secondary antibody and phycoerythrin-conjugated avidin (BD Pharmingen). The stained cells were analysed by flow cytometry (FACSCalibur, BD). Cell viability after 24-h treatment with bis-chloroethylnitrosourea (100 μg/ml; Sigma-Aldrich), pyridone 6 (0.5 μM; Calbiochem), and DAPT (100 nM; Sigma) was determined by flow cytometry using cells double-stained with Annexin V-fluorescein isothiocyanate (1:100; BD Pharmingen) and propidium iodide (50 μg/ml; Sigma-Aldrich).

## Bioinformatics analyses

The relative expression of IRFs was obtained from the Repository of Molecular Brain Neoplasia Data (REMBRANDT) database of the National Cancer Institute (http://caintegrator-info.nci.nih.gov/rembrandt). Relative probe signals were converted into heatmaps with Heatmap Builder 1.1 software. The REMBRANDT database was also used to determine correlations between clinical characteristics, survival and gene expression in glioma specimens. In these data, the term 'all gliomas' indicates all specimens that were used to analyse patient survival. The 'High expression group $\geqslant 2.0\times$' consisted of patients with gene expression $\geqslant$2-fold higher than mean values in normal tissue, whereas 'intermediate expression group' consisted of those with gene expression between that of 'high expression group $\geqslant 2.0\times$' and 'low expression group $\leqslant 2.0\times$'. In this study, the 'low expression group $\leqslant 2.0\times$' consisted of only 21 patients, so we excluded this group from data analysis.

## Mouse models

Nude mice (BALB/c nu/nu) were anaesthetized by intraperitoneal injection of a mixture of xylazine (Rompun; Bayer) and zolazepam (Zoletil 20; Virbac). For mouse brain orthotopic implantation, $5 \times 10^4$ cells were stereotactically injected into the left striata (coordinates: anterior–posterior, +2; medial–lateral, +2; dorsal–ventral, −2 mm from bregma; $n = 3$). For subcutaneous cell implantation, $10^6$ cells were subcutaneously injected into the mice ($n = 4$). For the mouse survival study, $1 \times 10^3$ cells were orthotopically implanted into the mice ($n = 6$). A mouse model of wound healing was established as described previously (Hofer *et al*., 1998) with a minor modification. Nude mice were anaesthetized by intraperitoneal injection of a mixture of xylazine and zolazepam. After making a 2-cm incision, subcutaneous tissue and muscles were removed from the buttock of each mouse. Human glioma cells or rat C6 cells ($1 \times 10^5$) admixed with Matrigel™ were injected into the wound site, and the resulting tumours were collected after 11 weeks (for human glioma cells) or 19 days (for rat C6 cells). All mouse experiments were approved by the animal care committee at the College of Life Science and Biotechnology, Korea University, and were performed in accordance with government and institutional guidelines and regulations.

## Statistics

Results of the multi-data set experiments were compared by analysis of variance using the Statistical Package for the Social Sciences software (version 12.0; SPSS); $P < 0.05$ or $P < 0.01$ were considered significant. Results of the two-data set experiments were compared by two-tailed Student's *t*-test; $P < 0.05$ or $P < 0.01$ was considered significant.

# Results

## Interferon regulatory factor 7 promotes brain tumours with increased angiogenesis and cell heterogeneity

To investigate the role of the inflammatory signalling in brain tumours, we first analysed the expression of the nine IRF family members (IRF1–IRF9) in different brain tumour types by mining the REMBRANDT database. Among the nine IRFs, IRF7, which is considered a master regulator of inflammation (Honda *et al*., 2005), was over-expressed >3-fold (on average) in astrocytomas ($n = 64$) and glioblastomas ($n = 152$) compared with non-tumour tissues ($n = 28$) (Supplementary Fig. 1A). These findings suggest the involvement of IRF7 in brain tumour pathology. Additionally, IRF7 messenger RNA levels were elevated in A172 and LN229 glioma cell lines (Supplementary Fig. 1B).

To understand the tumorigenic role of IRF7, we generated U87MG cells over-expressing IRF7 (U87MG-IRF7) and IRF7-depleted LN229 cells (LN229-shIRF7) (Fig. 1A, inset). IRF7 over-expression significantly increased tumour formation, whereas IRF7 knockdown markedly reduced tumorigenesis in subcutaneous xenograft models but did not significantly change cell growth *in vitro* (Fig. 1A and B; Supplementary Fig. 1C). Notably, CD31-positive vessel areas were substantially increased in U87MG-IRF7-driven tumours, whereas they were decreased in LN229-shIRF7-driven tumours (Fig. 1C). This finding suggests that IRF7 accelerates tumorigenicity in part by inducing angiogenesis but not by activating proliferation. In contrast to U87MG-driven subcutaneous tumours consisting primarily of S100β$^+$ glioma cells, U87MG-IRF7-driven tumours consisted of various cell populations, including the less abundant Nestin$^+$ and CD133$^+$ cells, as well as Tuj1$^+$ glioma cells and S100β$^+$ glioma cells (Fig. 1D), indicating tumour cell heterogeneity (Stiles and Rowitch, 2008; Shackleton *et al*., 2009). We then examined whether IRF7 regulates resistance to chemotherapy such as bis-chloroethylnitrosourea treatment. We found that IRF7 over-expression in U87MG cells reduced bis-chloroethylnitrosourea-induced cell death, whereas IRF7 depletion in LN229 cells increased bis-chloroethylnitrosourea sensitivity (Supplementary Fig. 1D), implying that IRF7 may play a role in chemotherapy resistance in cancer cells.

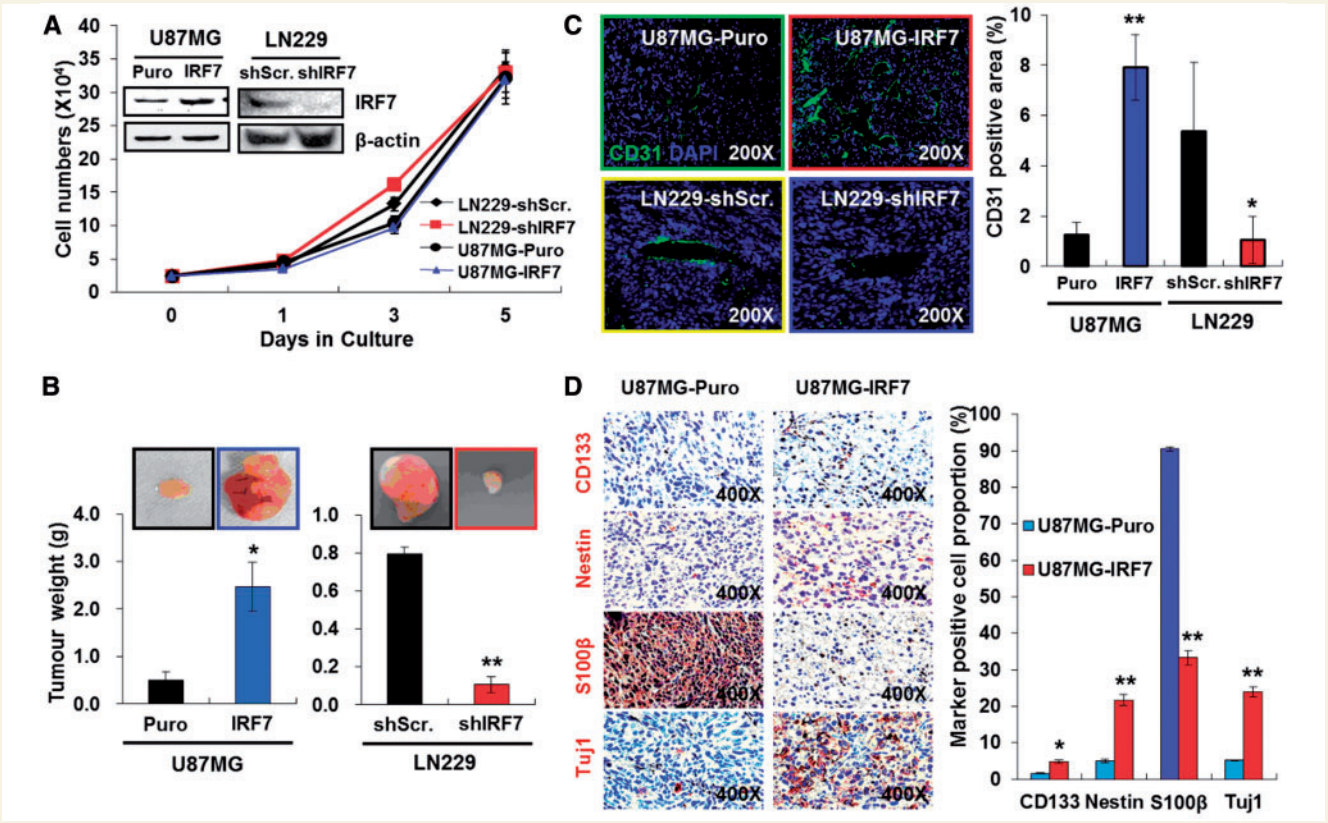


**Figure 1** IRF7 induces tumorigenicity with increased angiogenesis and cell heterogeneity. (**A**) Cell proliferation of U87MG-IRF7, LN229-shIRF7 and their corresponding control cells grown in Dulbecco's modified Eagle's medium with 10% foetal bovine serum for the indicated times. IRF7 over-expression in U87MG cells and short hairpin RNA-mediated IRF7 knockdown in LN229 cells were examined by western blot analysis (*inset*). (**B**) Increased tumour formation by ectopic IRF7 expression in U87MG cells (*left*) and decreased tumorigenesis by IRF7 depletion in LN229 cells (*right*) ($n = 4$). $^{*}P < 0.05$, $^{**}P < 0.01$. (**C**) Tumour vessel formation determined by immunostaining tumour tissues with CD31 antibody (green). Tumour vessels were significantly increased in U87MG-IRF7-driven tumours but markedly decreased in LN229-shIRF7-driven tumours. $^{*}P < 0.05$, $^{**}P < 0.01$. (**D**) Subcutaneous tumours derived from U87MG-IRF7 cells, but not U87MG control cells, included heterogeneous cell populations, such as $CD133^{+}$ and $Nestin^{+}$ GSCs, $S100\beta^{+}$ glioma cells and $Tuj1^{+}$ glioma cells. $^{*}P < 0.05$, $^{**}P < 0.01$.

## Interferon regulatory factor 7 promotes angiogenesis and heterogeneity by inducing cytokine expression

A custom angiogenesis antibody array was incubated with conditioned medium obtained from U87MG control cells and U87MG-IRF7 cells to identify the angiogenesis factors regulated by IRF7. We found that U87MG-IRF7 cells showed substantially increased secretion and messenger RNA levels of IL6, CXCL1 (Sager *et al*., 1992) and CCL2 (Deshmane *et al*., 2009) (Fig. 2A and B; Supplementary Fig. 2A and B). Since the IL6, CXCL1 and CCL2 promoters contain relatively conserved *cis*-elements for IRF7, NFκB and IRF3 (Supplementary Fig. 2C), we performed a chromatin immunoprecipitation assay to determine their binding affinities. We found that IRF7 and NFκB, but not IRF3, showed high binding affinities for their cognate sequences on the CXCL1 and CCL2 promoters, suggesting the regulation of CXCL1 and CCL2 transcription by both IRF7 and NFκB in U87MG-IRF7 cells (Fig. 2C). In contrast, IRF7 and IRF3 exhibited high binding affinities for their respective cognate sequences on the IL6 promoter, whereas NFκB did not bind to the IL6 promoter, implying that IL6 transcription is regulated by IRF7 and IRF3 in U87MG-IRF7 cells (Fig. 2C). Results from cell culture and xenograft experiments also demonstrated an increase in IL6 secretion and messenger RNA levels in U87MG-IRF7 cells and its reduction in IRF7-depleted LN229-shIRF7 cells (Fig. 3A and B; Supplementary Fig. 3A). Finally, the results of luciferase reporter assays showed that IRF7 induced IL6 promoter activity in a dose-dependent manner (Supplementary Fig. 3B).

To investigate the role of IRF7 and its target cytokines in tumour angiogenesis, we performed *in vitro* migration and tube formation assays using the conditioned medium obtained from U87MG-puro-shScramble, U87MG-CXCL1-shScramble, U87MG-IL6-shScramble, U87MG-CCL2-shScramble, U87MG-IRF7 shScramble, U87MG-IRF7-shCXCL1, U87MG-IRF7-shIL6 and U87MG-IRF7-shCCL2 cell lines (Supplementary Fig. 3C and D). We found that CXCL1 depletion in IRF7-overexpressing

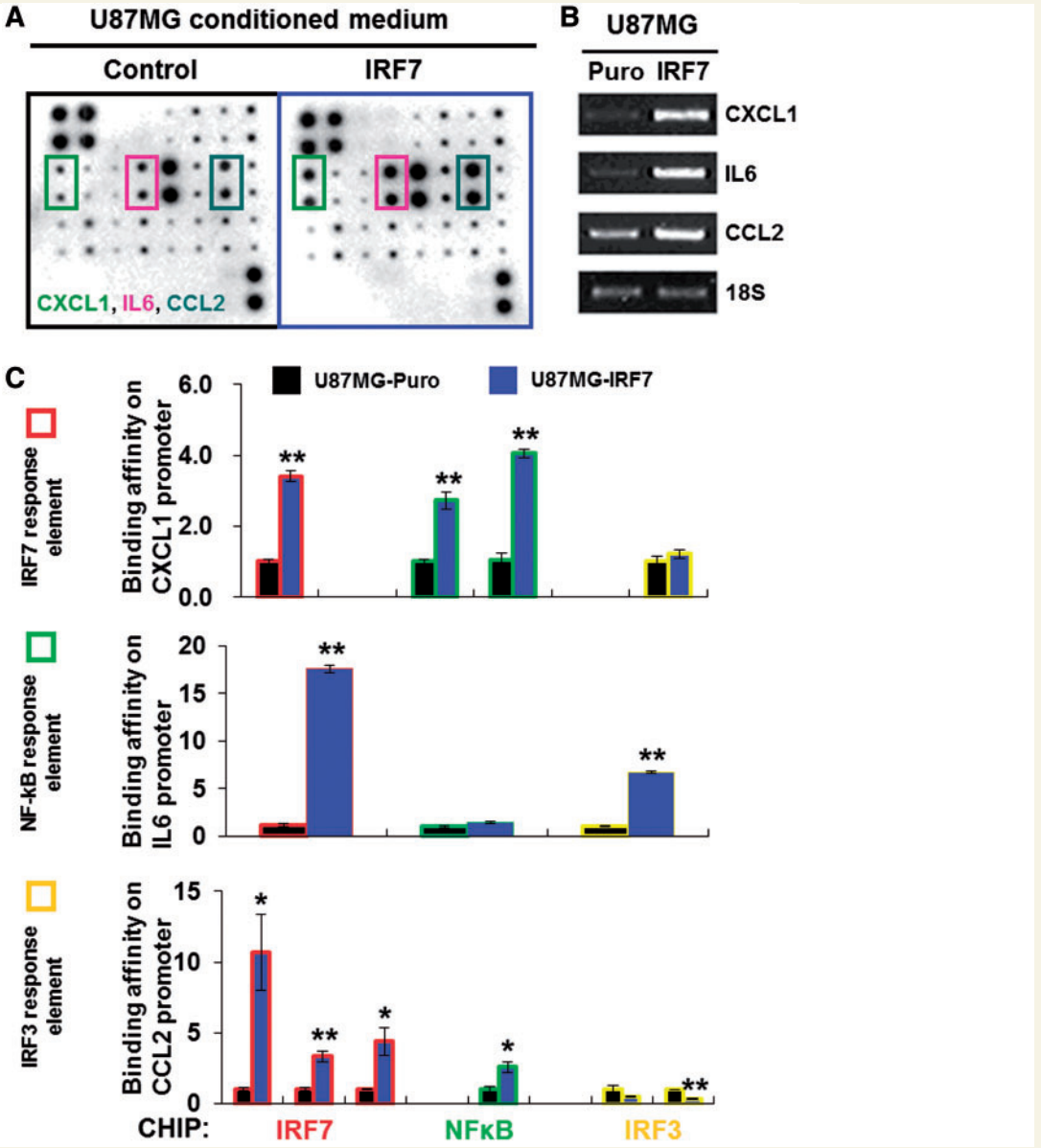


**Figure 2** IRF7 regulates cytokine expression. (**A**) Results from an angiogenesis cytokine antibody array revealed that ectopic expression of IRF7 increased secretion of IL6, CXCL1 and CCL2 in U87MG cells. (**B**) Semi-quantitative reverse transcriptase–polymerase chain reaction analysis showed upregulated CXCL1, IL6 and CCL2 messenger RNA levels in U87MG-IRF7 cells. (**C**) The chromatin immunoprecipitation assay was performed to determine the binding affinities of IRF7, NFkB and IRF3 to their cognate binding elements in CXCL1, IL6 and CCL2 promoters.

cells (U87MG-IRF7-shCXCL1) inhibited human brain vascular endothelial cell migration (Fig. 3C), whereas IRF7 and its three target cytokines induced tube formation of human brain vascular endothelial cells (Fig. 3D).

Ectopic expression of IRF7 or IL6 in U87MG cells accelerated tumour formation in mouse brain and subcutaneous xenograft tumour models, whereas IL6 knockdown in U87MG-IRF7 cells dramatically suppressed tumour formation (Fig. 4A and Supplementary Fig. 4), indicating a crucial role for IL6 in IRF7-driven tumorigenesis. In addition, we observed microglia ($F4/80^+$) infiltration of U87MG-IRF7-driven tumours but not U87MG-IL6-driven tumours (Fig. 4A). Similar to *in vivo* microglia migration, microglia migration was enhanced by IRF7, CXCL1 and CCL2, but not IL6 (Fig. 4B).

Since U87MG-IRF7-driven tumours consisted of cell populations expressing stem cell markers as well as cell populations expressing markers of differentiation (Fig. 1D), we examined whether the ectopic expression of IRF7 and IL6 in U87MG cells gives rise to GSC traits. We found that the tumoursphere-forming ability, a GSC feature (Singh *et al.*, 2003; Vescovi *et al.*, 2006), was markedly increased in U87MG-IRF7 and U87MG-IL6 cells grown in neural stem cell culture conditions (Lee *et al.*, 2006) (Fig. 4C). Depletion of IL6 in U87MG-IRF7 cells led to the most significant decrease in tumoursphere formation (Fig. 4C). Furthermore, GSC

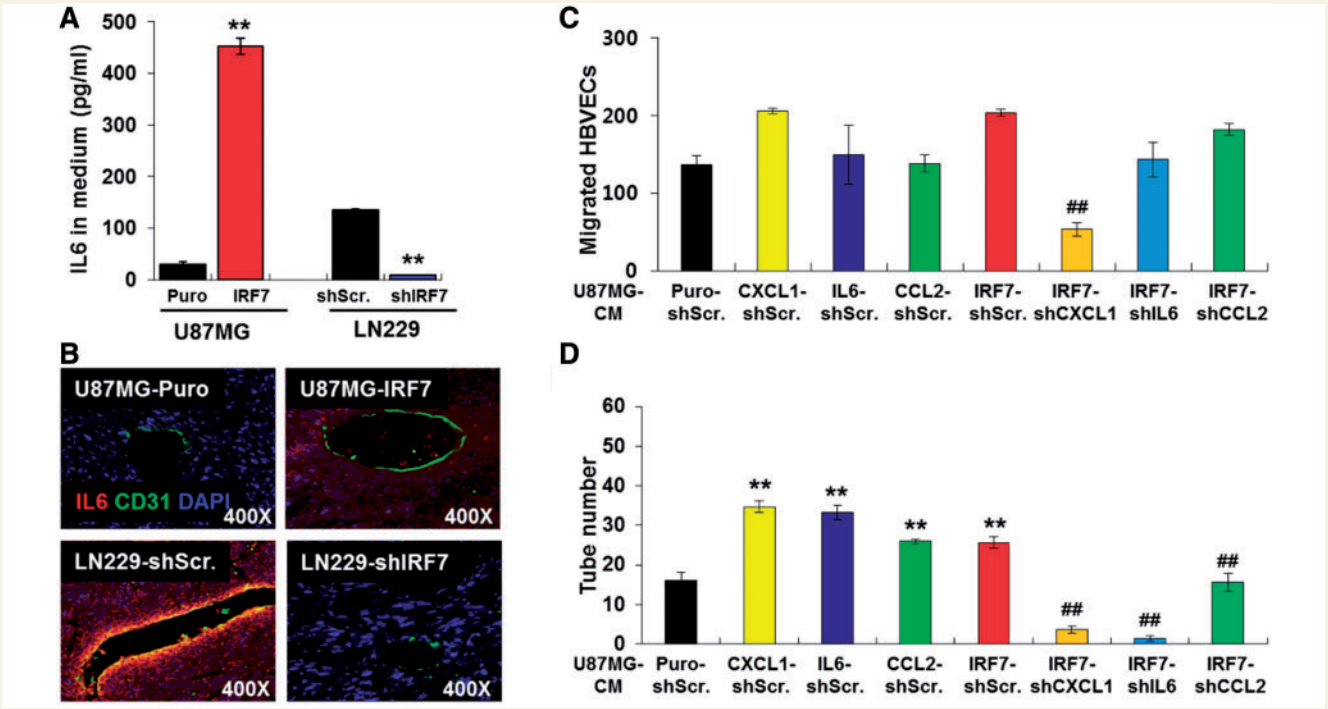


**Figure 3** IRF7 promotes tumour angiogenesis. (**A**) Enzyme linked immunosorbent assay analysis revealed that IL6 secretion was increased in U87MG-IRF7 cells and decreased in LN229-shIRF7 cells. $^{**}P < 0.01$. (**B**) Representative immunofluorescence images show increased and decreased IL6 expression with well-shaped CD31$^+$ endothelial vessels in tumours derived from U87MG-IRF7 and LN229-shIRF7 cells, respectively. Red = IL6; green = CD31; blue = DAPI-stained nuclei. 200× magnification. (**C**) *In vitro* migration assay of human brain vascular endothelial cells (HBVECs) revealed that ectopic expression of IRF7 or CXCL1 in U87MG cells enhanced human brain vascular endothelial cell migration. In addition, CXCL1-knockdown in U87MG-IRF7 cells markedly reduced human brain vascular endothelial cell migration. Conditioned medium from IRF7-overexpressing cells versus conditioned medium from cytokine-knockdown cells: $^{\#\#}P < 0.01$. (**D**) Tube numbers were significantly increased in human brain vascular endothelial cells grown in conditioned medium derived from IL6-, CXCL1- and CCL2-overexpressing U87MG cells. Conditioned medium from control cells versus conditioned medium from cytokine-overexpressing cells: $^{**}P < 0.01$; IRF7-overexpressing cells versus cytokine-knockdown cells: $^{\#\#}P < 0.01$.

proportions (CD133$^+$, Nestin$^+$ and Sox2$^+$ cells) increased with the over-expression of IRF7 and IL6 but decreased in the IL6-depleted U87MG-IRF7 cells (Supplementary Fig. 5C). We also found that the number of tumourspheres gradually increased in U87MG-IRF7 and to a lesser extent in U87MG-IL6 cells during three consecutive passages, indicating their self-renewal potential (Fig. 4D). Taken together, these findings indicate that IRF7 promotes tumour progression and cancer stemness of glioma cells by inducing IL6, suggesting a more important role in cancers than previously reported (Rolhion *et al*., 2001).

## Interferon regulatory factor 7-interleukin 6 signalling confers cancer stemness to glioma cells through JAK-STAT-mediated activation of Jagged-Notch signalling

Our group and others have demonstrated that Notch signalling plays a crucial role in brain cancer stem cell genesis, and IL6 stimulates Janus kinase-signal transducer and activator of transcription (JAK-STAT3)-Notch signalling in breast cancer mammospheres (Sansone *et al*., 2007; Jeon *et al*., 2008). Thus, we asked whether IRF7 induction of IL6 gives rise to brain cancer stem cell genesis through JAK-STAT3-mediated Notch activation. We suppressed the activation of JAK, STAT3 and Notch in U87MG-IRF7 and U87MG-IL6 cells using pharmacological inhibitors (JAK inhibitor pyridone 6, STAT3 inhibitor peptide, and DAPT, which indirectly inhibits Notch through $\gamma$-secretase inhibition). Our results showed that the tumoursphere-forming activity of U87MG-IRF7 and U87MG-IL6 cells was markedly suppressed by all three inhibitors (Fig. 5A) but did not significantly change cell viability (Supplementary Fig. 5A). In addition short hairpin RNA-mediated knockdown of IL6 in U87MG-IRF7 cells reduced IL6 secretion (Supplementary Fig. 3C), levels of phosphorylated STAT3 and Jagged1, tumoursphere formation, and stem cell proportion (Supplementary Fig. 5B–D). Furthermore, results of luciferase reporter assays revealed that IRF7 dose-dependently stimulated Jagged1 and CSL/Notch promoter activities, which were partially suppressed after JAK inhibitor (pyridone 6) treatment (Fig. 5B and C). The quantitative real-time polymerase chain reaction results showed that the increased messenger RNA levels of Jagged1 and two Notch-downstream targets (Hey1 and Hes1) (Iso *et al*.,

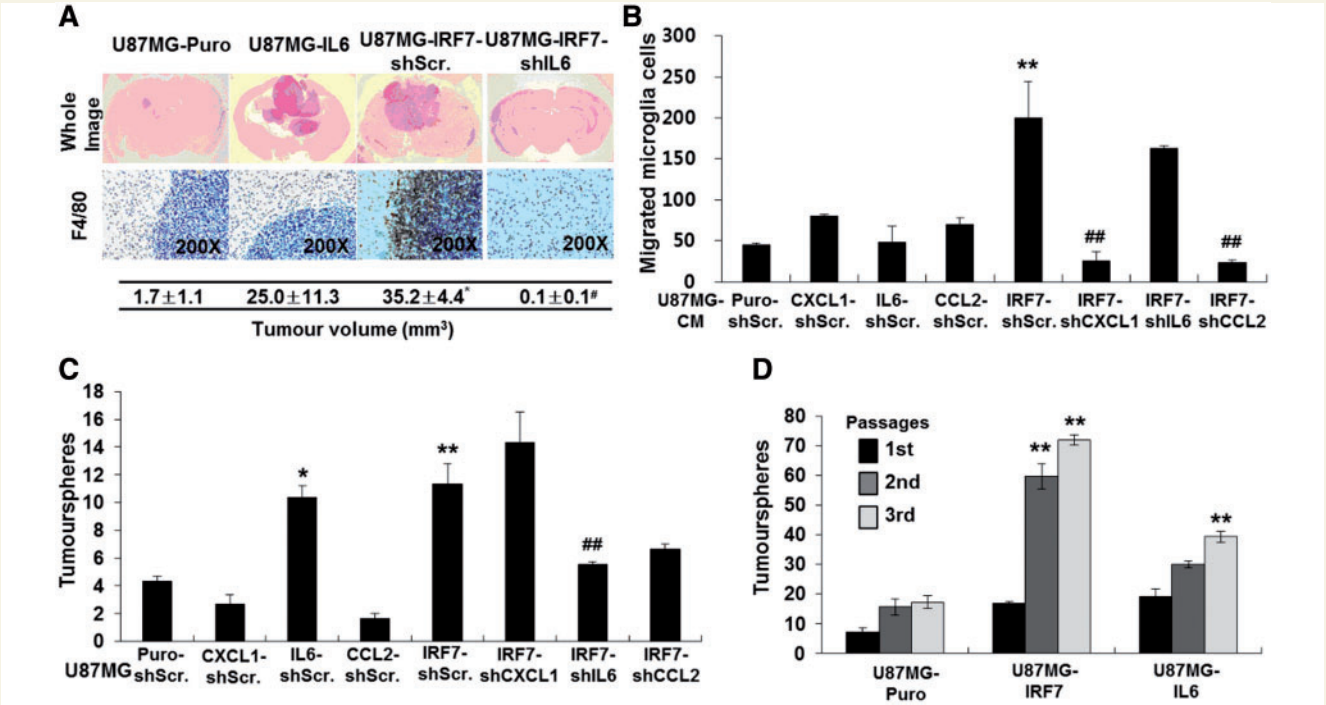


**Figure 4** IRF7 regulates microglial migration and tumour heterogeneity. (**A**) Brain tumour sections. No tumour was derived from U87MG-IRF7-shIL6 cells. Microglia infiltration was substantially increased in U87MG-IRF7-driven tumours (F4/80$^+$ microglial cells; 200× magnification). Tumour volume (mean ± SE) was determined by external measurement ($n = 3$). Control tumours versus IRF7-overexpressing tumours: $^*P < 0.05$; IRF7-overexpressing tumours versus IRF7-overexpressing/IL6-knockdown tumours: $^{\#}P < 0.05$. (**B**) Ectopic expression of IRF7, CXCL1 and CCL2 in U87MG cells stimulated microglia migration, whereas CXCL1-depleted U87MG-IRF7 cells markedly reduced microglia cell migration. Conditioned medium from control cells versus conditioned medium from IRF7 and three cytokines-overexpressing cells: $^{**}P < 0.01$; conditioned medium from IRF7-overexpressing cells versus conditioned medium from IRF7-overexpressing cells with depletion of each three cytokines -knockdown cells: $^{\#\#}P < 0.01$. (**C**) Ectopic expression of IRF7 or IL6 in U87MG cells enhanced tumoursphere formation when grown in neural stem cell culture conditions. Control cells versus IRF7-overexpressing cells: $^{**}P < 0.01$; IRF7-overexpressing cells versus IRF7-overexpressing/IL6-knockdown cells: $^{\#\#}P < 0.01$. (**D**) U87MG-IRF7 and U87MG-IL6 cells exhibited self-renewal potential to maintain their stemness during three consecutive passages. Passage 1 cells versus Passage 2/3 cells (in individual cell lines): $^{**}P < 0.01$.

2003) in U87MG-IRF7 and U87MG-IL6 cells were diminished by pyridone 6 treatment (Fig. 5D), indicating that IRF7 confers cancer stemness to glioma cells by stimulating Jagged-Notch signalling through IL6-JAK/STAT signalling.

## Interferon regulatory factor 7 expression in human patient-derived glioma stem cells and brain tumours

We further demonstrated the role of IRF7-IL6-Notch signalling in maintaining cancer stemness using several GSCs (X01, X02, X03, GSC3, GSC4 and GSC5) (Joo *et al*., 2008; Soeda *et al*., 2008) derived from patients with gliomas. IRF7 messenger RNA levels were strongly increased in all six GSCs compared with normal human astrocytes (Fig. 6A), and the protein levels of IRF7, phosphorylated STAT3 and Jagged1 were also increased in X02, X03 and GSC4 cells (Fig. 6B). Furthermore, inhibiting JAK/STAT-Notch signalling with pharmacological inhibitors (pyridone 6, STAT3 inhibitor and DAPT, respectively) sharply reduced the tumoursphere formation of X03, GSC4 and GSC8 cells (Fig. 6C). We found that although IRF7 was not directly associated with cell proliferation, as judged by no consistent growth alterations in the IRF7-depleted X03 and GSC8 cells (Supplementary Fig. 6A and B), IRF7 depletion significantly reduced IL6 and CCL2 expression (Fig. 6D), inactivated STAT-Notch signalling (Fig 6E and Supplementary Fig. 6C), and suppressed tumoursphere formation (Fig. 6F). Furthermore, IRF7 depletion in the GSCs led to a reduction in GSC proportion and GSC marker expression, but an increase in differentiated glioma cell proportion and differentiation lineage marker expression (Fig. 6G and Supplementary Fig. 6D), indicating that sustained IRF7 expression is necessary to prevent GSC differentiation.

To further assess the role of IL6 in IRF7-driven tumorigenesis in primary GSCs derived from patients with glioblastoma multiforme, we established GSC8-shIRF7-IL6 cells by transduction of IL6 in IRF7-depleted GSC8 cells (Supplementary Fig. 6E). Orthotopic injection of GSC8-shScramble, GSC8-shIRF7 and GSC8-shIRF7-IL6 cells into nude mice showed that IRF7 depletion significantly prolonged survival in tumour-bearing mice, whereas the

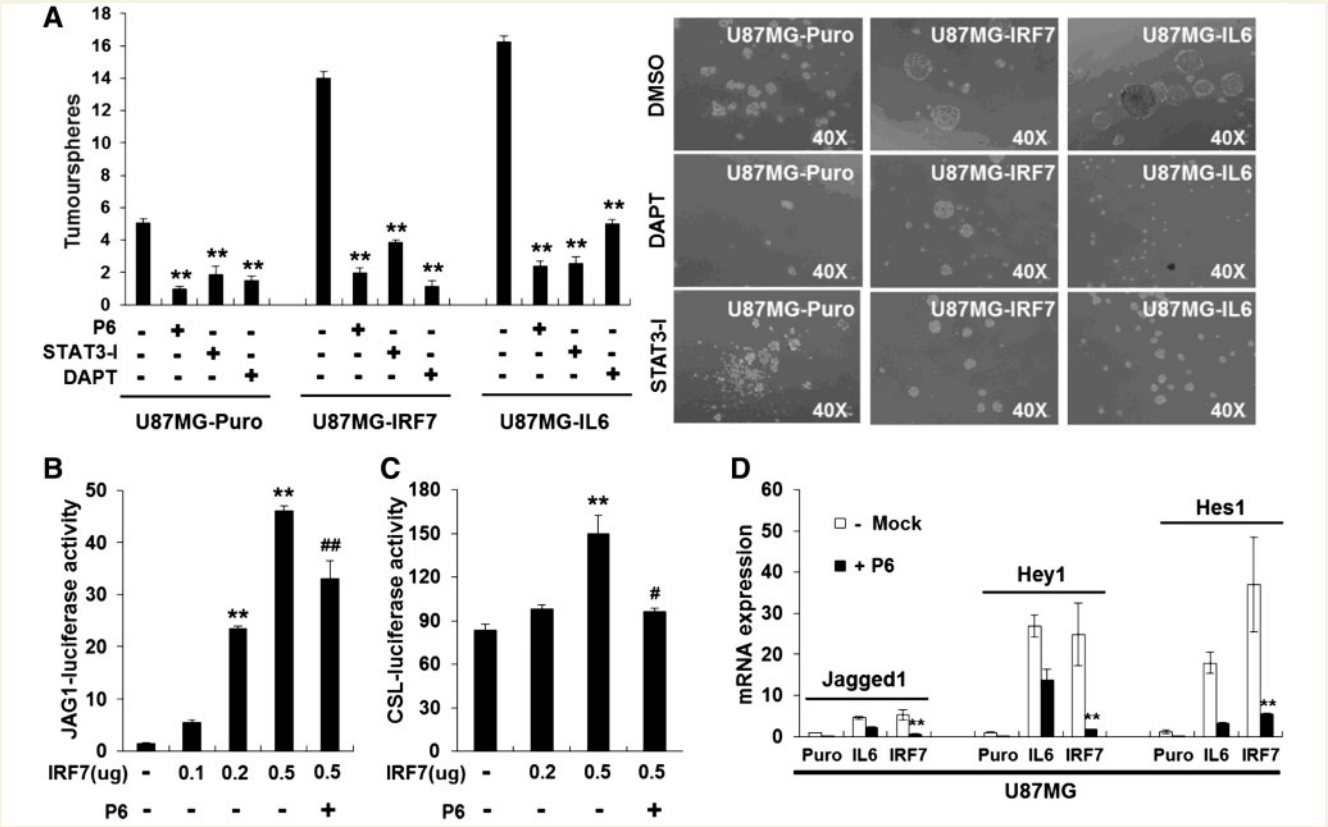


**Figure 5** IRF7–IL6 signalling promotes GSC self-renewal through Notch signalling. (**A**) JAK, STAT3 and Notch inhibitors suppressed tumoursphere formation (>10 μm) in U87MG-IL6 and U87MG-IRF7 cells. Representative tumourspheres (*right*). Control cells versus inhibitor-treated cells (in individual cell lines): $^{**}P < 0.01$. Luciferase reporter assays showed that the Jagged1 promoter (**B**) and CSL/Notch promoter (**C**) are induced by IRF7 over-expression, but are suppressed by JAK inhibitor (pyridone 6) treatment. Control cells versus IRF7-overexpressing cells: $^{**}P < 0.01$; IRF7-overexpressing cells versus pyridone 6-treated/IRF7-overexpressing cells: $^{\#}P < 0.05$, $^{\#\#}P < 0.01$. (**D**) The quantitative real-time polymerase chain reaction analysis revealed that Jagged1, Hey1 and Hes1 messenger RNA levels were reduced in U87MG-IL6 and U87MG-IRF7 cells by JAK inhibitor treatment (pyridone 6). Control cells versus pyridone 6-treated cells (in individual cell lines): $^{**}P < 0.01$.

reconstitution of IL6 in the IRF7-depleted GSCs dramatically accelerated death (Fig. 6H), indicating that IL6 signalling in the GSCs plays a crucial role in IRF7-driven tumorigenicity.

To identify upstream signals, we evaluated IRF7 expression in GSCs (GSC3, GSC4, X01 and X02) exposed to classic and putative glioma-related cytokines including epidermal growth factor, basic fibroblast growth factor, platelet-derived growth factor (Kesari and Stiles, 2006), transforming growth factor (TGF)β (Penuelas *et al*., 2009), leukaemia inhibitory factor (Penuelas *et al*., 2009), IL6, tumour necrosis factor α (TNFα), IL1β and lipopolysaccharide. We found that IRF7 expression was considerably increased in all these cell lines by TNFα (Fig. 7A). TNFα is one of the best characterized inducers of inflammatory signal transduction (Locksley *et al*., 2001) and is secreted by astrocytes and microglial cells in pathological conditions affecting the brain (Chung and Benveniste, 1990; Bruce *et al*., 1996). To investigate whether surgical wounds accelerate glioma progression through TNFα-IRF7 signalling, we transplanted rat C6 glioma cells into a mouse wound healing model that exhibits a well-documented inflammatory microenvironment (Martin and Leibovich, 2005; Gurtner *et al*., 2008) and found that tumour growth was accelerated (Supplementary Fig. 7A). Additionally, the increased TNFα and macrophage infiltration observed in these tumours were associated with IRF7 induction (Supplementary Fig. 7B). To further validate the biological effect of IRF7 on tumour progression in the inflammatory microenvironment, we subcutaneously transplanted LN229-shScramble and LN229-shIRF7 cells in wounded and non-wounded mice, and found that LN229-shScramble control cells, but not LN229-shIRF7 cells, markedly increased tumour formation in the wounded mice (Fig. 7B). Immunofluorescence analysis revealed that TNFα, IRF7, Jagged1, IL6, phosphorylated STAT3, Nestin and CD31 levels were substantially higher in LN229-shScramble-driven tumours than in LN229-shIRF7-driven tumours in the wounded mice (Fig. 7C and D). Furthermore, we found that IRF7 knockdown in the wounded mice decreased microglia infiltration (representative photos showing F4/80$^+$ cells in Fig. 7C and quantitative data in Fig. 7E) and GSC enrichment (representative photos showing CD133$^+$ cells in Fig. 7C and quantitative data in Fig. 7F). These findings suggest that IRF7 is regulated by the pathological inflammatory environment, and that TNFα-IRF7 signalling may play a crucial role in glioma recurrence after surgery.

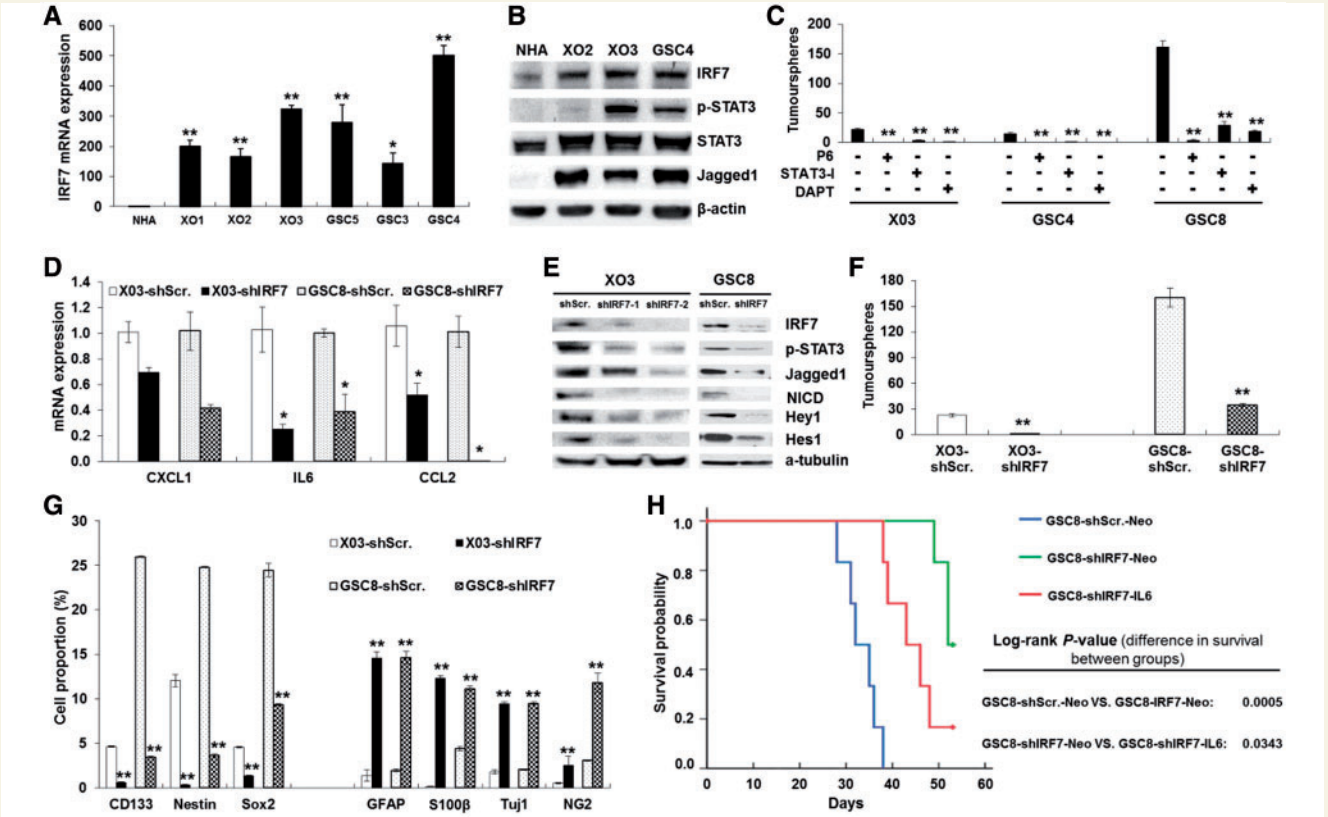


**Figure 6** Validation of IRF7–IL6-Notch signalling in human patient-derived GSCs. (**A**) The quantitative real-time polymerase chain reaction results showed that IRF7 messenger RNA was over-expressed in six GSCs established from patients with glioma. Normal human astrocytes (NHA) versus GSCs: $*P < 0.05$ or $**P < 0.01$. (**B**) Western blot analysis revealed that X02, X03 and GSC4 cells over-expressed IRF7, phosphorylated STAT3, and Jagged1 proteins. (**C**) JAK, STAT3 and Notch inhibitors suppress tumoursphere formation (>10 μm) in X03, GSC4 and GSC8 cells. Control cells versus inhibitor-treated cells (in individual cell lines): $**P < 0.01$. (**D**) The messenger RNA levels of IRF7-induced cytokines (IL6, CXCL1 and CCL2) in X03-shIRF7 cells, GSC8-shIRF7 cells, and their corresponding controls. $*P < 0.05$. (**E**) IRF7 knockdown in X03 and GSC8 cells reduced phosphorylated STAT3, Jagged1, active Notch intracellular domain (NICD), Hey1, and Hes1 protein levels. (**F**) Tumoursphere formation in X03-shIRF7, GSC8-shIRF7 and their corresponding controls. $**P < 0.01$. (**G**) Fluorescence-activated cell sorting analysis was performed to determine $CD133^+$, $Nestin^+$, $Sox2^+$, $GFAP^+$, $S100\beta^+$, $Tuj1^+$ and $NG2^+$ cell proportions in X03-shScramble, X03-shIRF7, GSC8-shScramble and GSC8-shIRF7 cells. $**P < 0.01$. (**H**) Kaplan–Meier survival rates of nude mice orthotopically injected with GSC8-shIRF7, GSC8-shIRF7-IL6 cells and GSC8 control cells ($n = 6$).

To determine the clinical importance of IRF7 expression in human brain tumours, we analysed IRF7 expression and found that IRF7 messenger RNA and protein levels were strongly increased in high-grade gliomas (WHO grade IV; $P < 0.05$) (Fig. 8A). Furthermore, data obtained from the REMBRANDT database showed that a 2-fold increase in IRF7 expression (120 of 204 patients) correlated with poor survival in patients with gliomas (Fig. 8B; $P < 0.01$). Interestingly, higher IRF7 expression was also significantly associated with patient clinical characteristics such as age (>40 years), glioma grade (WHO grade IV), and clinical score (<80% Karnofsky performance score), but not surgical resection (Table 1). To further assess the relationship between IRF7 expression and patient clinical characteristics, we performed multivariate analysis using the Cox proportional hazards regression model. As shown in Table 2, high IRF7 expression (hazard ratio 2.54; $P = 0.014$) and grade IV glioma (hazard ratio 3.28; $P = 0.003$) remained significant factors for poor survival after controlling for age, Karnofsky score and surgical resection, suggesting that IRF7 may serve as a prognostic factor for glioma patients.

In summary, we found that pathological inflammatory environments (e.g. surgical wounds) trigger IRF7 expression in gliomas through inflammatory cytokines (e.g. TNFα), thereby promoting IL6, CXCL1 and CCL2 expression and secretion (Fig. 8C). Secreted IL6 enables glioma cells to acquire GSC properties through JAK/STAT3-mediated activation of Jagged-Notch signalling, and stimulates tumour angiogenesis by inducing endothelial cell differentiation and vessel formation. Thus, the inflammatory microenvironment generated by TNFα–IRF7–IL6 signalling in glioma cells plays a crucial role in disease progression and glioblastoma formation through induction of GSC genesis and angiogenesis.

# Discussion

Interferon regulatory transcription factors appear to be important mediators of signals that sustain the inflammatory microenvironment necessary for tumour genesis and/or progression in many

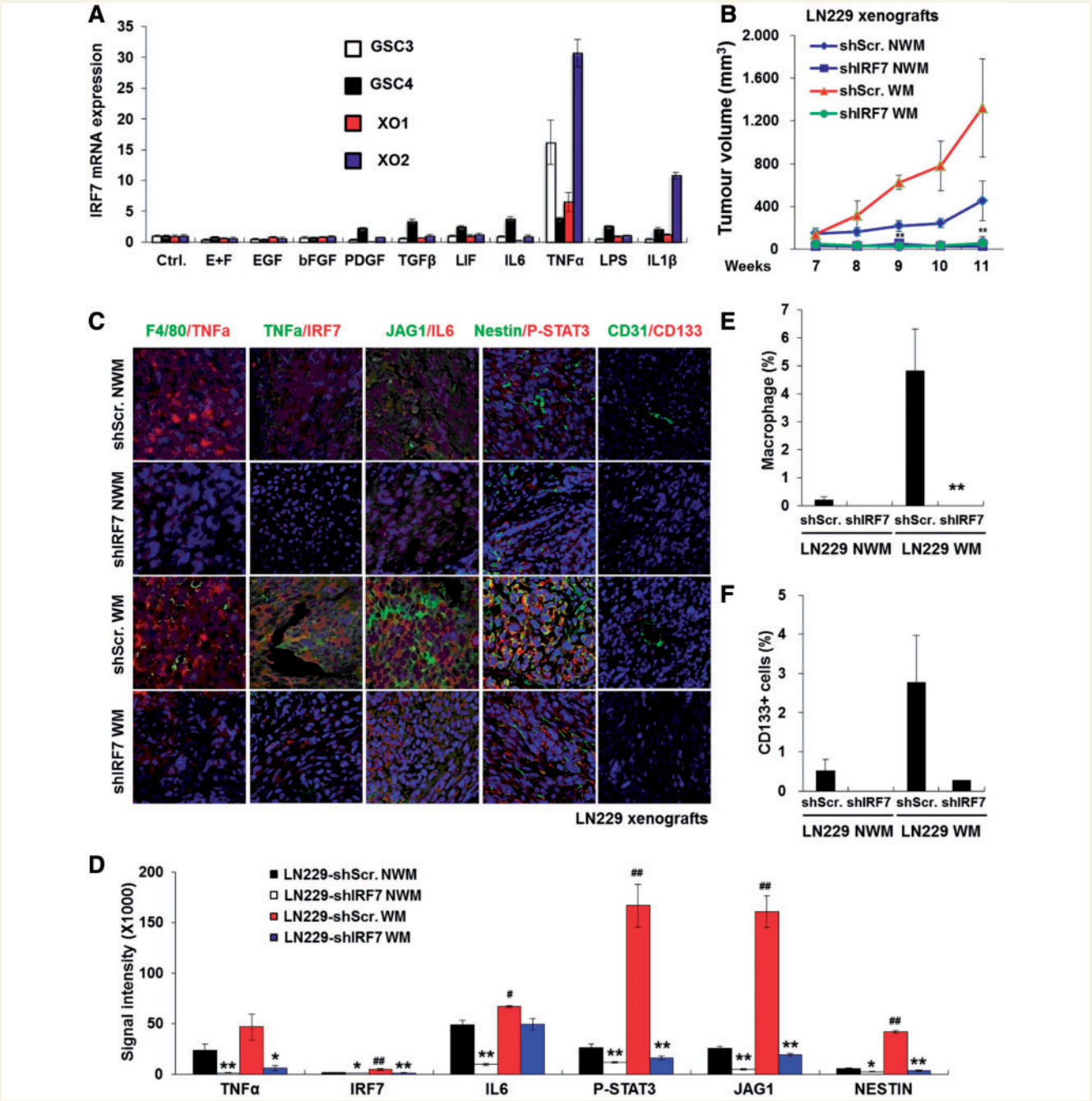


**Figure 7** IRF7 plays a central role in tumour progression and heterogeneity in a mouse model of wound healing. (**A**) IRF7 expression was strongly induced by TNF$\alpha$ in the various GSCs. E + F indicates treatment of epidermal growth factor and basic fibroblast growth factor. (**B**) Tumour growth of LN229 cells markedly increased when transplanted in wounded mice, but short hairpin RNA-mediated knockdown of IRF7 in LN229 cells markedly suppressed tumorigenesis. LN229-shScramble wound model versus LN229-shIRF7 wound model: $^{**}P < 0.01$. (**C**) Immunofluorescence images showing differential expression of TNF$\alpha$, IRF7, Jagged1, IL6, Nestin, phosphorylated STAT3, CD31 and CD133. (**D**) Quantitative analysis of signal intensities shown in (**C**). LN229-shScramble versus LN229-shIRF7: $^{*}P < 0.05$, $^{**}P < 0.01$; LN229-shScramble non-wound model versus LN229-shScramble wound model: $^{\#}P < 0.05$ or $^{\#\#}P < 0.01$. (**E**) Quantitative analysis of F4/80$^{+}$ cells infiltration in tumours shown in (**C**). LN229-shScramble wound model versus LN229-shIRF7 wound model: $^{**}P < 0.01$. (**F**) Quantification of CD133$^{+}$ GSCs in tumours shown in (**C**).

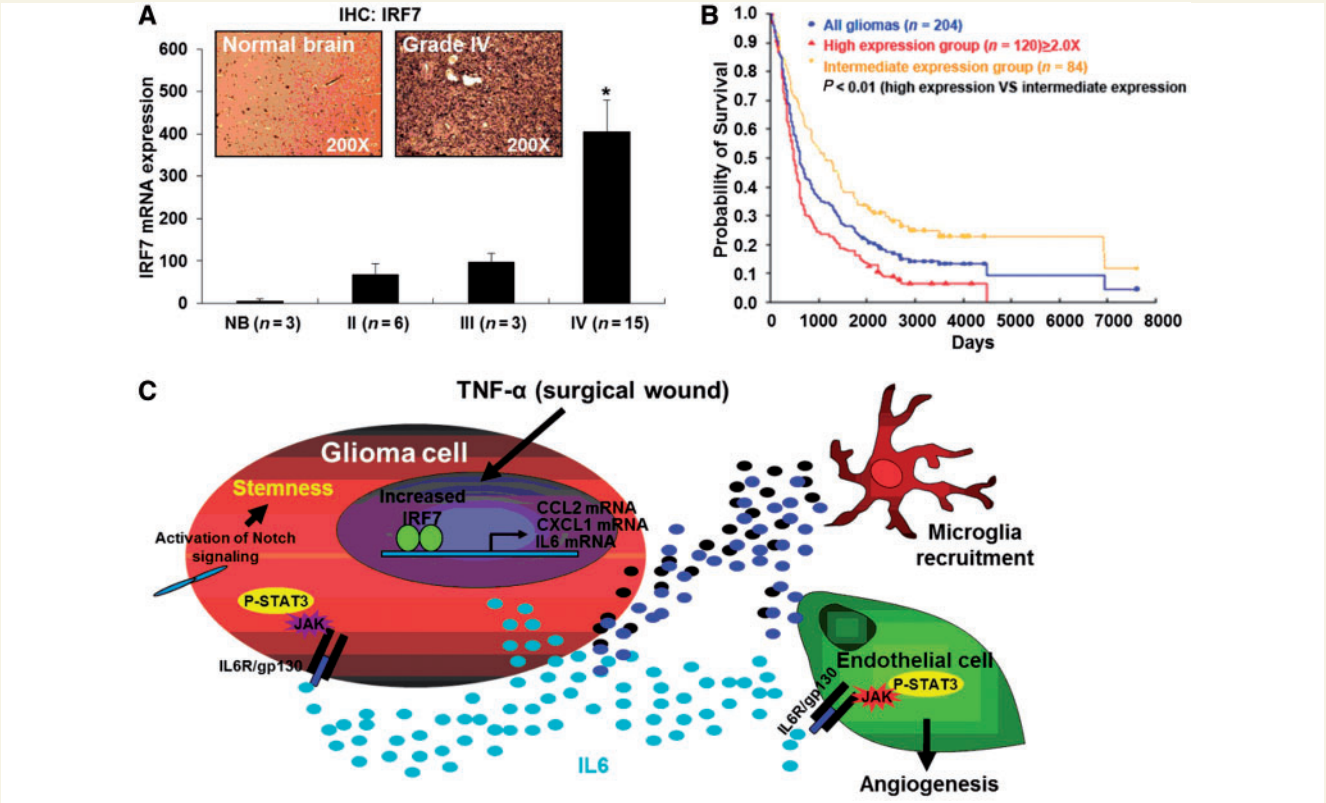


**Figure 8** IRF7 expression correlates with poor survival in patients with brain tumours. (**A**) Immunohistochemistry (IHC) results showing IRF7 expression in glioblastoma multiformes with matched normal brains. The quantitative real-time polymerase chain reaction results showed increased IRF7 expression in high-grade gliomas (WHO grade IV). Normal brain/grade II gliomas versus grade IV gliomas: $^*P < 0.05$. (**B**) IRF7 messenger RNA level correlates with poor patient survival. The high and intermediate IRF7 expression groups are described in the 'Materials and methods' section. (**C**) Schematic representation showing the role of TNF$\alpha$-IRF7-IL6 signalling in GSC genesis and angiogenesis in advanced and high-grade gliomas.

**Table 1 IRF7 expression levels and clinical characteristics in patients with brain tumours**

| Characteristics | Percentage of patients, *n* (%) | | *P*-value |
|---|---|---|---|
| | IRF7 high (*n* = 30) | IRF7 intermediate (*n* = 26) | |
| Age (years) | | | |
| <40 | 36 (8) | 64 (14) | <0.0001 |
| ⩾40 | 65 (22) | 35 (12) | |
| WHO grade | | | |
| I–III | 38 (11) | 62 (18) | <0.0001 |
| IV | 70 (19) | 30 (8) | |
| Karnofsky score | | | |
| <80 | 76 (18) | 24 (6) | <0.0001 |
| ⩾80 | 44 (12) | 56 (20) | |
| Extent of resection | | | |
| Partial resection | 56 (18) | 44 (14) | 0.4 |
| Complete resection | 40 (12) | 60 (12) | |

*P*-value was obtained using Pearson's chi-squared test. These data sets were obtained from the REMBRANDT database.

types of malignancies. However, there is little evidence supporting the role of IRF-driven inflammation in brain tumour pathogenesis. Although studies have demonstrated IRF7 over-expression in reactive hyperplastic lymph nodes, paediatric lymphoma and Epstein–Barr virus-transformed CNS lymphoma (Zhang *et al.*, 2004; Park *et al.*, 2007), neither study demonstrates a functional link between IRF7 expression and tumorigenesis. On the other hand, several lines of evidence support the role of IL6 as a primary mediator of the inflammatory response important in the pathogenesis of many types of malignancies (Hodge *et al.*, 2005; Rose-Jone *et al.*, 2006). Furthermore, recent studies have demonstrated the importance of IL6 in RAS- and epidermal growth factor receptor-mediated tumorigenesis, as well as the direct role of IL6-STAT signalling in an inflammatory model of *de novo* tumourigenesis (i.e. colitis-associated colon cancer) (Ancrile *et al.*, 2006; Gao *et al.*, 2007; Bollrath *et al.*, 2009; Grivennikov *et al.*, 2009). Moreover, increased IL6 levels in gliomas are associated with the grade of malignancy and contribute to the maintenance of tumour heterogeneity through paracrine cytokine signalling circuits in U87MG-EGFRvIII cells (Rolhion *et al.*, 2001;

**Table 2 Multivariate analysis of IRF7 expression and clinical characteristics of 56 glioma patients**

| | $R^2$ | Hazard ratio (95% CI) | *P*-value |
|---|---|---|---|
| Age (years) | | | |
| <40 versus ⩾40 | 0.48 | 1.62 (0.73–3.56) | 0.233 |
| WHO grade | | | |
| I–III versus IV | 1.188 | 3.28 (1.51–7.12) | 0.003 |
| Karnofsky score | | | |
| <80 versus ⩾80 | −0.089 | 0.92 (0.46–1.82) | 0.8 |
| Extent of resection | | | |
| Partial resection versus complete resection | 0.120 | 1.18 (0.57–2.24) | 0.732 |
| IRF7 expression | | | |
| Intermediate versus high | 0.932 | 2.54 (1.20–5.34) | 0.014 |

Multivariate analysis was carried out using the Cox proportional hazard model. These data sets were obtained from the REMBRANDT database. $R^2$ = co-efficient of determination; 95% CI = 95% confidence interval.

Tchirkov *et al*., 2007; Wang *et al*., 2009; Inda *et al*., 2010). Our findings suggest that the overexpression of both IRF7 and IL6 in U87MG cells accelerates glioma formation by stimulating angiogenesis and Jagged/Notch-dependent acquisition of GSC properties.

Angiogenesis is a hallmark of cancer and the inflammatory response (Carmeliet and Jain, 2000; Hanahan and Weinberg, 2011). Recent studies have described a perivascular niche microenvironment in which endothelial-derived nitric oxide regulates the maintenance of GSC features through Notch signalling (Calabrese *et al*., 2007; Charles *et al*., 2010). Therefore, our results strongly suggest that increased angiogenesis and activation of Notch signalling by IRF7-driven cytokines (IL6, CCL2 and CXCL1) play crucial roles in tumorigenicity and GSC genesis and maintenance. The upregulation of CCL2 and CXCL1 is also involved in GSC maintenance through recruitment of microglia, which further promotes the protumorigenic inflammatory microenvironment and angiogenesis by secreting additional angiogenic cytokines, such as TGFβ, IL8 and RANTES (Ghosh and Chaudhuri, 2010).

The difference between IRF7- and IL6-driven tumours is the infiltration of glioma cells into the brain parenchyma. Unlike tumours generated from U87MG-IRF7 cells, U87MG-IL6 cells give rise to gliomas with clear tumour margins in the brain. Given that recruitment of microglial cells in gliomas promotes tumour invasion and progression through membrane type I-matrix metalloproteinase expression, and CCL2 is involved in microglia cell migration (Markovic *et al*., 2009), we speculate that the increased CCL2 and CXCL1 secretion demonstrated by U87MG-IRF7 cells, but not U87MG-IL6 cells, may play a role in the recruitment of microglial cells into the invasive edge of tumours, further stimulating the diffusive infiltration of tumour cells into the surrounding parenchymal tissue.

Developmental regulators such as Id4 and Olig2 appear to play direct roles in GSC genesis (Ligon *et al*., 2007; Jeon *et al*., 2008). However, no studies have shown that inflammatory regulators are involved in GSC genesis and maintenance. The results reported here demonstrate that IRF7 is directly involved in promoting stem-like properties in glioma cells. Conversely, IRF7 depletion in GSCs diminishes self-renewal and increases differentiation. Similar to our previous study showing that Id4-induced activation of Jagged/Notch signalling is sufficient to convert Ink4a/Arf$^{-/-}$ astrocytes to glioma stem-like cells (Jeon *et al*., 2008), the IRF7-driven acquisition and maintenance of GSC properties is also mediated by Jagged/Notch through IL6-JAK/STAT signalling. These findings suggest that deregulation of IRF7-IL6-Jagged/Notch signalling may be an important event in tumour progression in many types of malignancies, including inflammation-associated cancers. Therefore, further investigation of this important signalling pathway in a variety of tumours will be particularly valuable for the development of new therapeutic agents and modalities.

## Acknowledgements

The authors would like to thank Dr Dong Seok Lee for providing microglial cells and Dr. Akio Soeda for providing X01, X02, X03 glioma stem cells.

## Funding

National R&D Program for Cancer Control, Ministry of Health and Welfare, Republic of Korea (grant number 1020270); Brain Korea 21 project funded by the Ministry of Education, Science, and Technology of Korea (post-doctoral fellowship to X.J.); National Research Foundation of Korea funded by MEST (NRF-2009-351-C00137) (post-doctoral fellowship programme to S.H.K.); H.M.J is a recipient of the Best Graduate Student Scholarship from Korea University.

## Supplementary material

Supplementary material is available at *Brain* online.

# References


Ancrile B, Lim KH. Counter conditioned medium. Oncogenic Ras-induced secretion of IL6 is required for tumorigenesis. Genes Dev 2007; 21: 1714–9.

Bollrath J, Phesse TJ, von Burstin VA, Putoczki T, Bennecke M, Bateman T, et al. gp130-mediated Stat3 activation in enterocytes regulates cell survival and cell-cycle progression during colitis-associated tumorigenesis. Cancer Cell 2009; 15: 91–102.

Bruce AJ, Boling W, Kindy MS, Peschon J, Kraemer PJ, Carpenter MK, et al. Altered neuronal and microglial responses to excitotoxic and ischemic brain injury in mice lacking TNF receptors. Nat Med 1996; 2: 788–94.

Calabrese C, Poppleton H, Kocak M, Hogg TL, Fuller C, Hamner B, et al. A perivascular niche for brain tumor stem cells. Cancer Cell 2007; 11: 69–82.

Carmeliet P, Jain PK. Angiogenesis in cancer and other diseases. Nature 2000; 407: 249–57.

Charles N, Ozawa T, Squatrito M, Bleau AM, Brennan CW, Hambardzumyan D, et al. Perivascular nitric oxide activates notch signaling and promotes stem-like character in PDGF-induced glioma cells. Cell Stem Cell 2010; 6: 141–52.

Chung IY, Benveniste EN. Tumor necrosis factor-alpha production by astrocytes. Induction by lipopolysaccharide, IFN-gamma, and IL-1 beta. J Immunol 1990; 144: 2999–3007.

Coffelt SB, Hughes R, Lewis CE. Tumor-associated macrophages: Effectors of angiogenesis and tumor progression. Biochim Biophys Acta 2009; 1796: 11–8.

Deshmane SL, Kremlev S, Amini S, Sawaya BE. Monocyte chemoattractant protein-1 (MCP-1): an overview. J Interferon Cytokine Res 2009; 29: 313–26.

Gao SP, Mark KG, Leslie K, Pao W, Motoi N, Gerald WL, et al. Mutations in the EGFR kinase domain mediate STAT3 activation via IL-6 production in human lung adenocarcinomas. J Clin Invest 2007; 117: 3846–56.

Ghosh A, Chaudhuri S. Microglial action in glioma: a boon turns bane. Immunol Lett 2010; 131: 3–9.

Grivennikov S, Karin E, Terzic J, Mucida D, Yu GY, Vallabhapurapu S, et al. IL-6 and Stat3 are required for survival of intestinal epithelial cells and development of colitis-associated cancer. Cancer Cell 2009; 15: 103–13.

Gurtner GC, Werner S, Barrandon Y, Longaker MT. Wound repair and regeneration. Nature 2008; 453: 314–20.

Hanahan D, Weinberg RA. Hallmarks of cancer: the next generation. Cell 2011; 144: 646–74.

Hodge DR, Hurt EM, Farrar WL. The role of IL-6 and STAT3 in inflammation and cancer. Eur J Cancer 2005; 41: 2502–12.

Hofer SO, Shrayer D, Reichner JS, Hoekstra HJ, Wanebo HJ. Wound-induced tumor progression: a probable role in recurrence after tumor resection. Arch Surg 1998; 41: 383–9.

Honda K, Taniguchi T. IRFs: master regulators of signalling by Toll-like receptors and cytosolic pattern-recognition receptors. Nat Rev Immunol 2006; 6: 644–58.

Honda K, Yanai H, Negishi H, Asagiri M, Sato M, Mizutani T, et al. IRF-7 is the master regulator of type-I interferon-dependent immune responses. Nature 2005; 434: 772–7.

Inda MM, Bonavia R, Mukasa A, Narita Y, Sah DW, Vandenberg S, et al. Tumor heterogeneity is an active process maintained by a mutant EGFR-induced cytokine circuit in glioblastoma. Genes Dev 2010; 24: 1731–45.

Iso T, Kedes L, Hamamori Y. HES and HER*P* families: multiple effectors of the Notch signaling pathway. J Cell Physiol 2003; 194: 237–55.

Jeon HM, Jin X, Lee JS, Oh SY, Sohn YW, Park HJ, et al. Inhibitor of differentiation 4 drives brain tumor-initiating cell genesis through cyclin E and notch signaling. Genes Dev 2008; 22: 2028–33.

Joo KM, Kim SY, Jin X, Song SY, Kong DS, Lee JI, et al. Clinical and biological implications of CD133-positive and CD133-negative cells in glioblastomas. Lab Invest 2008; 88: 808–15.

Kesari S, Stiles CD. The bad seed: PDGF receptors link adult neural progenitors to glioma stem cells. Neuron 2006; 51: 151–3.

Kim TK, Lee JS, Oh SY, Jin X, Choi YJ, Lee TH, et al. Direct transcriptional activation of promyelocytic leukemia protein by IFN regulatory factor 3 induces the p53-dependent growth inhibition of cancer cells. Cancer Res 2007; 67: 11133–40.

Lee J, Kotliarova S, Kotliarov Y, Li A, Su Q, Donin NM, et al. Tumor stem cells derived from glioblastomas cultured in bFGF and EGF more closely mirror the phenotype and genotype of primary tumors than do serum-cultured cell lines. Cancer Cell 2006; 9: 391–403.

Ligon KL, Huillard E, Mehta S, Kesari S, Liu H, Alberta JA, et al. Olig2-regulated lineage-restricted pathway controls replication competence in neural stem cells and malignant glioma. Neuron 2007; 53: 503–17.

Locksley RM, Killeen N, Lenardo MJ. The TNF and TNF receptor superfamilies integrating mammalian biology. Cell 2001; 104: 487–501.

Mantovani A. Cancer: Inflaming metastasis. Nature 2009; 457: 36–7.

Mantovani A, Allavena P, Sica A, Balkwill F. Cancer-related inflammation. Nature 2008; 454: 436–44.

Markovic DS, Vinnakota K, Chirasani S, Synowitz M, Raguet H, Stock K, et al. Gliomas induce and exploit microglial MT1-MM*P* expression for tumor expansion. Proc Natl Acad Sci USA 2009; 106: 12530–5.

Martin P, Leibovich SJ. Inflammatory cells during wound repair: the good, the bad and the ugly. Trends Cell Biol 2005; 15: 599–607.

Park HS, Kim YJ, Bae YK, Lee NH, Lee YJ, Hah JO, et al. Differential expression patterns of IRF3 and IRF7 in pediatric lymphoid disorders. Int J Biol Markers 2007; 22: 34–8.

Panne D, Maniatis T, Harrison SC. An atomic model of the interferon-beta enhanceosome. Cell 2007; 129: 1111–23.

Pedranzini L, Dechow T, Berishaj M, Comenzo R, Zhou P, Azare J, Bornmann W, Bromberg J. Pyridone 6, a pan-Janus-activated kinase inhibitor, induces growth inhibition of multiple myeloma cells. Cancer Res 2006; 66: 9714–21.

Penuelas S, Anido J, Prieto-Sanchez RM, Folch G, Barba I, Cuartas I, Garcia-Dorado D, et al. TGF-β increases glioma-initiating cell self-renewal through the induction of LIF in human glioblastoma. Cancer Cell 2009; 15: 315–27.

Pollard SM, Yoshikawa K, Clarke ID, Danovi D, Stricker S, Russell R, et al. Glioma stem cell lines expanded in adherent culture have tumor-specific phenotypes and are suitable for chemical and genetic screens. Cell Stem Cell 2009; 4: 568–80.

Rolhion C, Penault-Llorca F, Kémény JL, Lemaire JJ, Jullien C, Labit-Bouvier C, et al. Interleukin-6 overexpression as a marker of malignancy in human gliomas. J Neurosurg 2001; 94: 97–101.

Rose-John S, Scheller J, Elson G, Jones SA. Interleukin-6 biology is coordinated by membrane-bound and soluble receptors: role in inflammation and cancer. J Leukoc Biol 2006; 80: 227–36.

Sager R, Haskill S, Anisowicz A, Trask D, Pike MC. GRO: a novel chemotactic cytokine. Adv Ex*P* Med Biol 1991; 305: 73–7.

Sansone P, Storci G, Tavolari S, Guarnieri T, Giovannini C, Taffurelli M, et al. IL-6 triggers malignant features in mammospheres from human ductal breast carcinoma and normal mammary gland. J Clin Invest 2007; 117: 3988–4002.

Shackleton M, Quintana E, Fearon ER, Morrison SJ. Heterogeneity in cancer: cancer stem cells versus clonal evolution. Cell 2009; 138: 822–9.

Singh SK, Clarke ID, Terasaki M, Bonn VE, Hawkins C, Squire J, et al. Identification of a cancer stem cell in human brain tumors. Cancer Res 2003; 63: 5821–8.

Soeda A, Inagaki A, Oka N, Ikegame Y, Aoki H, Yoshimura S, et al. Epidermal growth factor plays a crucial role in mitogenic regulation of human brain tumor stem cells. J Biol Chem 2008; 283: 10958–66.

Son MJ, Woolard K, Nam DH, Lee J, Fine HA. SSEA-1 is an enrichment marker for tumor-initiating cells in human glioblastoma. Cell Stem Cell 2009; 4: 440–52.

Stiles C, Rowitch D. Glioma stem cells: a midterm exam. Neuron 2008; 58: 832–46.

Tchirkov A, Khalil T, Chautard E, Mokhtari K, Véronèse L, Irthum B, et al. Interleukin-6 gene amplification and shortened survival in glioblastoma patients. Br J Cancer 2007; 96: 474–6.

Turkson J, Ryan D, Kim JS, Zhang Y, Chen Z, Haura E, et al. Phosphotyrosyl peptides block Stat3-mediated DNA binding activity, gene regulation, and cell transformation. J Biol Chem 2001; 276: 45443–55.

Vescovi A, Galli R, Reynolds B. Brain tumour stem cells. Nat Rev Cancer 2006; 6: 425–36.

Wang H, Lathia JD, Wu Q, Wang J, Li Z, Heddleston JM, et al. Targeting interleukin-6 signaling suppresses glioma stem cell survival and tumor growth. Stem Cells 2009; 27: 2393–404.

Zhang L, Zhang J, Lambert Q, Der CJ, Del Valle L, Miklossy J, et al. Interferon regulatory factor 7 is associated with Epstein-Barr virus-transformed central nervous system lymphoma and has oncogenic properties. J Virol 2004; 78: 12987–95.

Zheng Y, Lin L, Zheng Z. TGF-alpha induces upregulation and nuclear translocation of Hes1 in glioma cell. Cell Biochem Funct 2008; 26: 692–700.